Figure 7.26 shows that for lasers with small mode volumes, i.e. mode volumes of the size of the wavelength cubed, the threshold is no longer well defined.

7.9 Short pulse generation by Q-Switching

The energy stored in the laser medium can be released suddenly by increasing the Q-value of the cavity so that the laser reaches threshold. This can be done actively, for example by quickly moving one of the resonator mirrors in place or passively by placing a saturable absorber in the resonator [**?**, 8]. Hellwarth first suggest this method only one year after the invention of the laser. As a rough orientation for a solid-state laser the following relation for the relevant time scales is generally valid

$$\tau_L \gg T_R \gg \tau_p. \tag{7.59}$$

7.9.1 Active Q-Switching

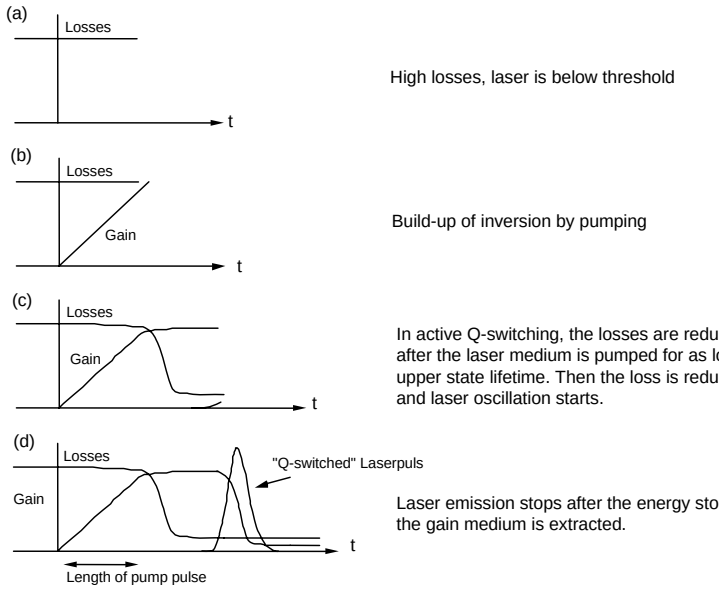

Figure 7.27: Gain and loss dynamics of an actively Q-switched laser.

Fig. 7.27 shows the principle dynamics of an actively Q-switched laser. The laser is pumped by a pump pulse with a length on the order of the upper-state lifetime, while the intracavity losses are kept high enough so that the laser can not reach threshold. At this point, the laser medium acts as energy storage with the energy slowly relaxing by spontaneous and nonradiative transitions. Intracavity loss is suddenly reduced, for example by a rotating cavity mirror. The laser is pumped way above threshold and the light field builts exponentially up until the pulse energy comes close to the saturation energy of the gain medium. The gain saturates and its energy is extracted, causing the laser to be shut off by the pulse itself.

A typical actively Q-switched pulse is asymmetric: The rise time is proportional to the net gain after the Q-value of the cavity is actively switched to a high value. The light intensity grows proportional to $2g_0/T_R$. When the gain is depleted, the fall time mostly depends on the cavity decay time τ_p, see Figure 7.28. For short Q-switched pulses a short cavity length, high gain and a large change in the cavity Q is necessary. If the Q-switch is not fast, the pulse width may be limited by the speed of the switch. Typical time scales for electro-optical and acousto-optical switches are 10 ns and 50 ns, respectively

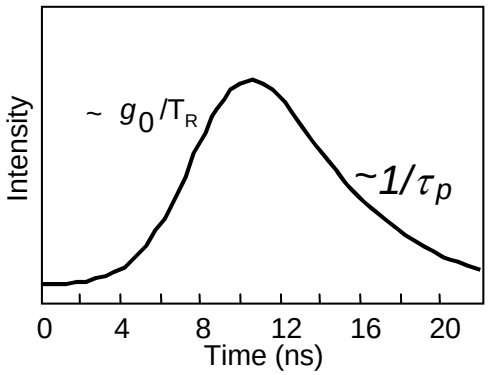

Figure 7.28: Asymmetric actively Q-switched pulse.

For example, with a diode-pumped Nd:YAG microchip laser [15] using an electro-optical switch based on $LiTaO_3$ Q-switched pulses as short as 270 ps at repetition rates of 5 kHz, peak powers of 25 kW at an average power of 34 mW, and pulse energy of 6.8 μJ have been generated (Figure 7.29).

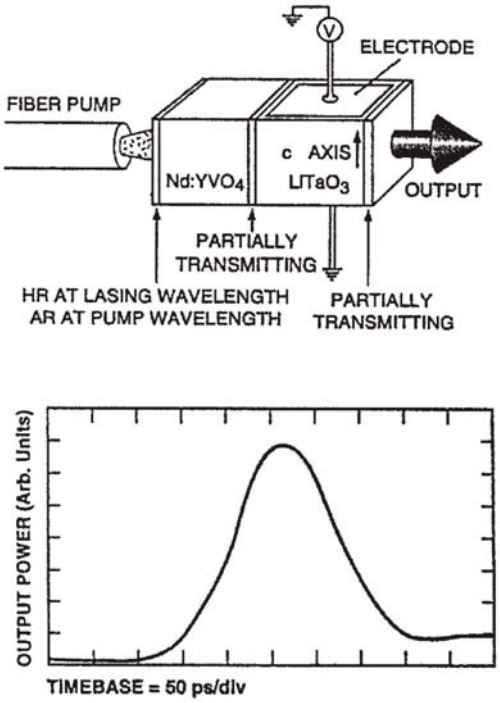

Figure 7.29: Q-switched microchip laser using an electro-optic switch. The pulse is measured with a sampling scope [15]

7.9.2 Passive Q-Switching

In the case of passive Q-switching, the intracavity loss modulation is performed by a saturable absorber, which introduces large losses for low intensities of light and small losses for high intensity.

Relaxation oscillations are due to a periodic exchange of energy stored in the laser medium by the inversion and the light field. Without the saturable absorber these oscillations are damped. If for some reason there is t0o much gain in the system, the light field can build up quickly. Especially for a low gain cross section the back action of the growing laser field on the inversion is weak and it can grow further. This growth is favored in the presence of loss that saturates with the intensity of the light. The laser becomes unstable and the field intensity growth as long as the gain does not saturate below the net loss, see Fig.7.30.

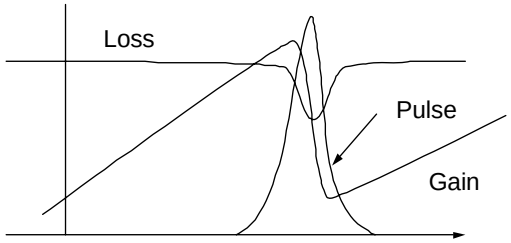

Figure 7.30: Gain and loss dynamics of a passively Q-switched laser

The saturable absorber leads to a destabilization of the relaxation oscillations resulting in the giant laser pulses.

7.10 Short pulse generation by mode locking

Q-switching is a single mode pheonomenon, i.e. the pulse build-up and decay occurs over many round-trips via build-up of energy and decay in a single (or a few) longitudinal mode. If one could get several longitudinal modes lasing in a phase coherent fashion with resepct to each other, these modes would be the Fourier components of a periodic pulse train emitted from the laser. Then a single pulse is traveling inside the laser cavity. This is called mode locking and the pulses generated are much shorter than the cavity round-trip time due to interference of the fields from many modes. The electric field can be written as a superpostion of the longitudinal modes. We neglect polarization for the moment.

$$E(z,t) = \Re\left[\sum_m \hat{E}_m e^{\mathrm{j}(\omega_m t - k_m z + \phi_m)}\right], \tag{7.60a}$$

$$\omega_m = \omega_0 + m\Delta\omega = \omega_0 + \frac{m\pi c}{\ell}, \tag{7.60b}$$

$$k_m = \frac{\omega_m}{c}. \tag{7.60c}$$

Equation (7.60a) can be rewritten as

$$E(z,t) = \Re\left\{ e^{\mathrm{j}\omega_0(t-z/c)} \sum_m \hat{E}_m e^{\mathrm{j}(m\Delta\omega(t-z/c)+\phi_m)} \right\} \tag{7.61a}$$

$$= \Re\left[A(t-z/c) e^{\mathrm{j}\omega_0(t-z/c)} \right] \tag{7.61b}$$

with the complex envelope

$$A\left(t-\frac{z}{c}\right) = \sum_m E_m e^{\mathrm{j}(m\Delta\omega(t-z/c)+\phi_m)} = \text{complex envelope (slowly varying).} \tag{7.62}$$

$e^{\mathrm{j}\omega_0(t-z/c)}$ is the carrier wave (fast oscillation). Here, both the carrier and the envelope travel with the same speed (no dispersion assumed). The envelope function is periodic with period

$$T = \frac{2\pi}{\Delta\omega} = \frac{2\ell}{c} = \frac{L}{c}, \tag{7.63}$$

where L is the optical round-trip length in the cavity. If we assume that N modes with equal amplitudes $E_m = E_0$ and equal phases $\phi_m = 0$ are lasing, the envelope is given by

$$A(z,t) = E_0 \sum_{m=-(N-1)/2}^{(N-1)/2} e^{\mathrm{j}(m\Delta\omega(t-z/c))}. \tag{7.64}$$

With

$$\sum_{m=0}^{q-1} a^m = \frac{1-a^q}{1-a}, \tag{7.65}$$

we obtain

$$A(z,t) = E_0 \frac{\sin\left[\frac{N\Delta\omega}{2}\left(t-\frac{z}{c}\right)\right]}{\sin\left[\frac{\Delta\omega}{2}\left(t-\frac{z}{c}\right)\right]}. \tag{7.66}$$

The laser intensity I is proportional to $E(z,t)^2$ averaged over one optical cycle: $I \sim |A(z,t)|^2$. At $z = 0$, we obtain

$$I(t) \sim |E_0|^2 \frac{\sin^2\left(\frac{N\Delta\omega t}{2}\right)}{\sin^2\left(\frac{\Delta\omega t}{2}\right)}. \tag{7.67}$$

The periodic pulses given by Eq. (7.67) have

- the period: $T = 1/\Delta f = L/c$
- pulse duration: $\Delta t = \frac{2\pi}{N\Delta\omega} = \frac{1}{N\Delta f}$
- peak intensity $\sim N^2|E_0|^2$
  - average intensity $\sim N|E_0|^2 \Rightarrow$ peak intensity is enhanced by a factor N.

If the phases of the modes are not locked, i.e. ϕ_m is a random sequence then the intensity fluctuates randomly about its average value ($\sim N|E_0|^2$), which is the same as in the mode-locked case. Figure 7.31 shows the intensity of a modelocked laser versus time,if the relative phases of the modes to each other is (a) constant and (b) random

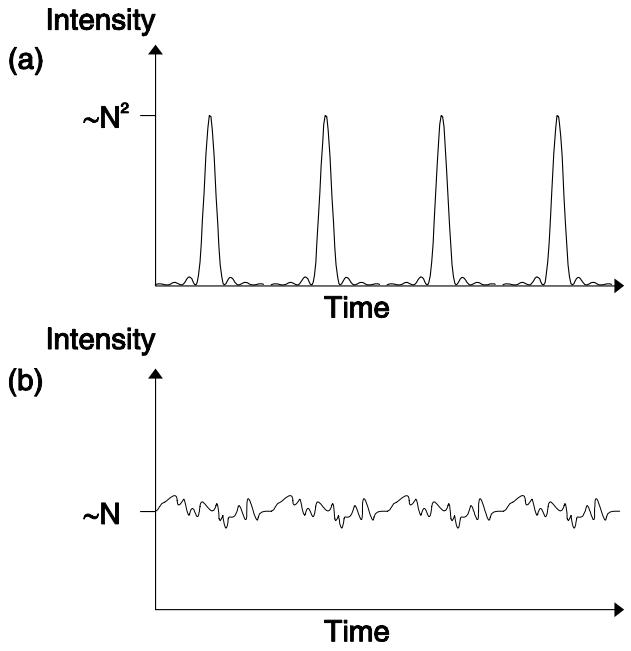

Figure 7.31: Laser intensity versus time from a mode-locked laser with (a) perfectly locked phases and (b) random phases.

We are distinguishing between active modelocking, where an external loss modulator is inserted in the cavity to generate modelocked pulses, and passive modelocking, where the pulse is modulating the intracavity itself via a saturable absorber.

7.10.1 Active Mode Locking

Active mode locking was first investigated in 1970 by Kuizenga and Siegman [16] and later by Haus [17] . In the approach by Haus, modelocking is treated as a pulse propagation problem.

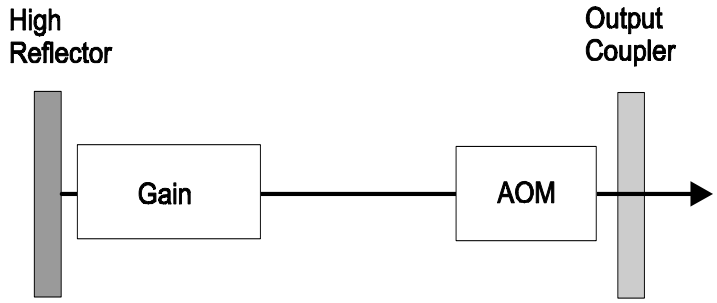

Figure 7.32: Actively modelocked laser with an amplitude modulator (Acousto-Optic-Modulator).

The pulse is shaped in the resonator by the finite bandwidth of the gain and the loss modulator, which periodically varies the intracavity loss according to $q(t) = M\left(1 - \cos(\omega_M t)\right)$. The modulation frequency has to be precisely tuned to the resonator round-trip time, $\omega_M = 2\pi/T_R$, see Fig.7.32. The mode locking process is then described by the master equation for the slowly varying pulse envelope

$$T_R \frac{\partial A}{\partial T} = \left[g(T) + D_g \frac{\partial^2}{\partial t^2} - l - M\left(1 - \cos(\omega_M t)\right) \right] A. \tag{7.68}$$

This equation can be interpreted as the total pulse shaping due to gain, loss and modulator within one roundtrip, see Fig.7.33.

If we fix the gain in Eq. (7.68) at its stationary value, what ever it might be, Eq.(7.68) is a linear p.d.e, which can be solved by separation of variables. The pulses, we expect, will have a width much shorter than the round-trip time T_R. They will be located in the minimum of the loss modulation where the cosine-function can be approximated by a parabola and we obtain

$$T_R \frac{\partial A}{\partial T} = \left[g - l + D_g \frac{\partial^2}{\partial t^2} - M_s t^2 \right] A. \tag{7.69}$$

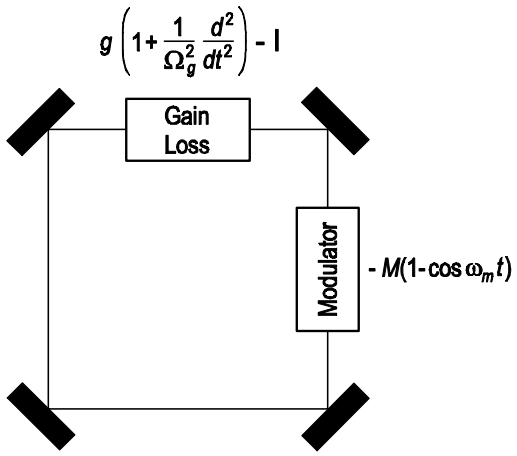

Figure 7.33: Schematic representation of the master equation for an actively mode-locked laser.

M_s is the modulation strength, and corresponds to the curvature of the loss modulation in the time domain at the minimum loss point

$$D_g = \frac{g}{\Omega_g^2}, \tag{7.70}$$

$$M_s = \frac{M\omega_M^2}{2}. \tag{7.71}$$

The differential operator on the right side of (7.69) corresponds to the Schrödinger-Operator of the harmonic oscillator problem. Therefore, the eigen functions of this operator are the Hermite-Gaussians

$$A_n(T,t) = A_n(t)e^{\lambda_n T/T_R}, \tag{7.72}$$

$$A_n(t) = \sqrt{\frac{W_n}{2^n\sqrt{\pi}n!\tau_a}}H_n(t/\tau_a)e^{-\frac{t^2}{2\tau_a^2}}, \tag{7.73}$$

where τ_a determines the pulse width of the Gaussian pulse. The width is given by the fourth root of the ratio between gain dispersion and modulator strength

$$\tau_a = \sqrt[4]{D_g/M_s}. \tag{7.74}$$

Note, from Eq. (7.72) we see that the gain per round-trip of each eigenmode

is given by λ_n (or in general the real part of λ_n), which is given by

$$\lambda_n = g_n - l - 2M_s\tau_a^2(n + \frac{1}{2}). \tag{7.75}$$

The corresponding saturated gain for each eigen solution is given by

$$g_n = \frac{1}{1 + \frac{W_n}{P_L T_R}}, \tag{7.76}$$

where W_n is the energy of the corresponding solution and $P_L = E_L/\tau_L$ the saturation power of the gain. Eq. (7.75) shows that for a given g the eigen solution with $n = 0$, the ground mode, has the largest gain per roundtrip. Thus, if there is initially a field distribution which is a superpostion of all eigen solutions, the ground mode will grow fastest and will saturate the gain to a value

$$g_s = l + M_s\tau_a^2. \tag{7.77}$$

such that $\lambda_0 = 0$ and consequently all other modes will decay since $\lambda_n < 0$ for $n \geq 1$. This also proves the stability of the ground mode solution [17]. Thus active modelocking without detuning between resonator round-trip time and modulator period leads to Gaussian steady state pulses with a FWHM pulse width

$$\Delta t_{FWHM} = 2\ln 2\tau_a = 1.66\tau_a. \tag{7.78}$$

The spectrum of the Gaussian pulse is given by

$$\tilde{A}_0(\omega) = \int_{-\infty}^{\infty} A_0(t)e^{i\omega t}dt \tag{7.79}$$

$$= \sqrt{\sqrt{\pi}W_n\tau_a}e^{-\frac{(\omega\tau_a)^2}{2}}, \tag{7.80}$$

and its FWHM is

$$\Delta f_{FWHM} = \frac{1.66}{2\pi\tau_a}. \tag{7.81}$$

Therfore, the time-bandwidth product of the Gaussian is

$$\Delta t_{FWHM} \cdot \Delta f_{FWHM} = 0.44. \tag{7.82}$$

The stationary pulse shape of the modelocked laser is due to the parabolic loss modulation (pulse shortening) in the time domain and the parabolic filtering (pulse stretching) due to the gain in the frequency domain, see Figs.

7.34 and 7.35. The stationary pulse is achieved when both effects balance. Since external modulation is limited to electronic speed and the pulse width does only scale with the inverse square root of the gain bandwidth actively modelocking typically only results in pulse width in the range of 10-100ps.

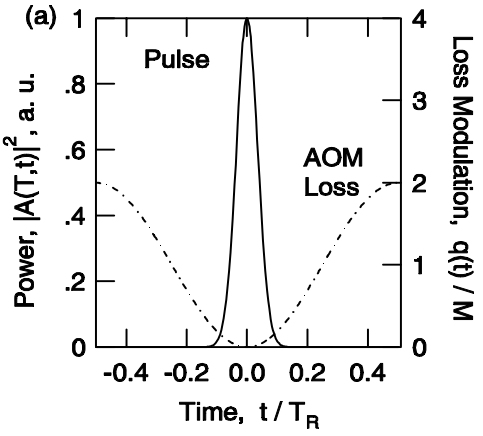

Figure 7.34: Loss modulation leads to pulse shortening in each roundtrip

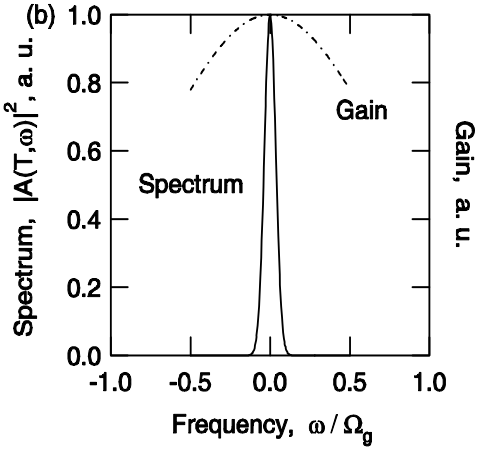

Figure 7.35: The finite gain bandwidth broadens the pulse in each roundtrip. For a certain pulse width there is balance between the two processes.

For example: Nd:YAG; $2l = 2g = 10\%$, $\Omega_g = \pi\Delta f_{FWHM} = 0.65$ THz,

$M = 0.2$, $f_m = 100$ MHz, $D_g = 0.24$ ps^2, $M_s = 4 \cdot 10^{16} s^{-1}$, $\tau_p \approx 99$ ps.

With the pulse width (7.74), Eq.(7.77) can be rewritten in several ways

$$g_s = l + M_s \tau_a^2 = l + \frac{D_g}{\tau_a^2} = l + \frac{1}{2} M_s \tau_a^2 + \frac{1}{2} \frac{D_g}{\tau_a^2}, \tag{7.83}$$

which means that in steady state the saturated gain is lifted above the loss level l, so that many modes in the laser are maintained above threshold. There is additional gain necessary to overcome the loss of the modulator due to the finite temporal width of the pulse and the gain filter due to the finite bandwidth of the pulse. Usually

$$\frac{g_s - l}{l} = \frac{M_s \tau_a^2}{l} \ll 1, \tag{7.84}$$

since the pulses are much shorter than the round-trip time. The stationary pulse energy can therefore be computed from

$$g_s = \frac{1}{1 + \frac{W_s}{P_L T_R}} = l. \tag{7.85}$$

The name modelocking originates from studying this pulse formation process in the frequency domain. Note, the term

$$-M \left[1 - \cos(\omega_M t)\right] A$$

generates sidebands on each cavity mode present according to

$$\begin{aligned} & -M \left[1 - \cos(\omega_M t)\right] \exp(j\omega_{n_0} t) \\ = \; & -M \left[\exp(j\omega_{n_0} t) - \frac{1}{2} \exp(j(\omega_{n_0} t - \omega_M t)) - \frac{1}{2} \exp(j(\omega_{n_0} t + \omega_M t))\right] \\ = \; & M \left[-\exp(j\omega_{n_0} t) + \frac{1}{2} \exp(j\omega_{n_0 - 1} t) + \frac{1}{2} \exp(j\omega_{n_0 + 1} t)\right] \end{aligned}$$

if the modulation frequency is the same as the cavity round-trip frequency. The sidebands generated from each running mode is injected into the neighboring modes which leads to synchronisation and locking of neighboring modes, i.e. mode-locking, see Fig.7.36

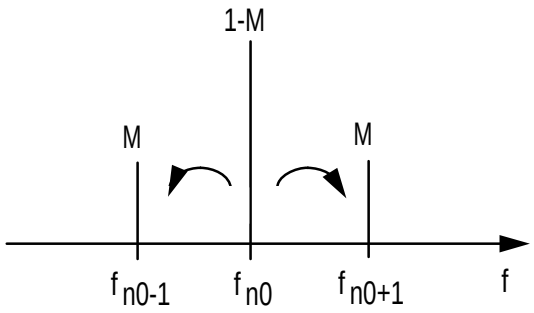

Figure 7.36: Modelocking in the frequency domain: The modulator transvers energy from each mode to its neighboring mode, thereby redistributing energy from the center to the wings of the spectrum. This process seeds and injection locks neighboring modes.

7.10.2 Passive Mode Locking

Electronic loss modulation is limited to electronic speeds. Therefore, the curvature of the loss modulation that determines the pulse length is limited. It is desirable that the pulse itself modulates the loss. The shorter the pulse the sharper the loss modulation and eventually much shorter pulses can be reached.

The dynamics of a laser modelocked with a fast saturable absorber can also be easily understood using the master equation (7.68) and replacing the loss due to the modulator with the loss from a saturable absorber. For a fast saturable absorber, the losses q react instantaneously on the intensity or power $P(t) = |A(t)|^2$ of the field

$$q(A) = \frac{q_0}{1 + \frac{|A|^2}{P_A}}, \tag{7.86}$$

where P_A is the saturation power of the absorber. Such absorbers can be made out of semiconductor materials or nonlinear optical effects can be used to create artificial saturable absorption, such as in Kerr lens mode locking.

There is no analytic solution of the master equation (7.68) when the loss modulation is replaced by the absorber response (7.86). We can however make expansions on the absorber response to get analytic insight. If the absorber is not saturated, we can expand the response (7.86) for small

intensities

$$q(A) = q_0 - \gamma|A|^2, \tag{7.87}$$

with the saturable absorber modulation coefficient $\gamma = q_0/P_A$. The constant nonsaturated loss q_0 can be absorbed in the losses $l_0 = l + q_0$. The resulting master equation is

$$T_R \frac{\partial A(T,t)}{\partial T} = \left[g - l_0 + D_f \frac{\partial^2}{\partial t^2} + \gamma|A|^2 \right] A(T,t). \tag{7.88}$$

Up to the imaginary unit, this equation is similar to a type of nonlinear Schroedinger Equation, i.e. the potential depends on the wave function itself. One finds as a possible stationary solution

$$A_s(T,t) = A_s(t) = A_0 \text{sech}\left(\frac{t}{\tau}\right). \tag{7.89}$$

Note, there is

$$\frac{d}{dx}\text{sech}x = -\tanh x \, \text{sech}x, \tag{7.90}$$

$$\begin{aligned} \frac{d^2}{dx^2}\text{sech}x &= \tanh^2 x \, \text{sech}x - \text{sech}^3 x, \\ &= \left(\text{sech}x - 2\,\text{sech}^3 x\right). \end{aligned} \tag{7.91}$$

Substitution of the solution (7.89) into the master equation (7.88), and assuming steady state, results in

$$\begin{aligned} 0 = &\left[(g - l_0) + \frac{D_f}{\tau^2}\left[1 - 2\text{sech}^2\left(\frac{t}{\tau}\right)\right]\right. \\ &\left. + \gamma|A_0|^2 \text{sech}^2\left(\frac{t}{\tau}\right)\right] \cdot A_0 \text{sech}\left(\frac{t}{\tau}\right). \end{aligned} \tag{7.92}$$

Comparison of the coefficients with the sech- and sech^3-expressions leads to a condition for the peak pulse intensity and pulse width, τ, and for the saturated gain

$$\frac{D_f}{\tau^2} = \frac{1}{2}\gamma|A_0|^2, \tag{7.93}$$

$$g = l_0 - \frac{D_f}{\tau^2}. \tag{7.94}$$

From Eq.(7.93) and with the pulse energy of a sech pulse

$$W = \int_{-\infty}^{+\infty} 2|A_s(t)|^2 dt = 2|A_0|^2\tau, \tag{7.95}$$

follows

$$\tau = \frac{4D_f}{\gamma W}. \tag{7.96}$$

$$g_s(W) = \frac{g_0}{1 + \frac{W}{P_L T_R}} \tag{7.97}$$

Equation (7.94) together with (7.96) determines the pulse energy

$$\begin{aligned} g_s(W) &= \frac{g_0}{1 + \frac{W}{P_L T_R}} = l_0 - \frac{D_f}{\tau^2} \\ &= l_0 - \frac{(\gamma W)^2}{16 D_g} \end{aligned} \tag{7.98}$$

Figure 7.37 shows the time dependent variation of gain and loss in a laser modelocked with a fast saturable absorber on a normalized time scale.

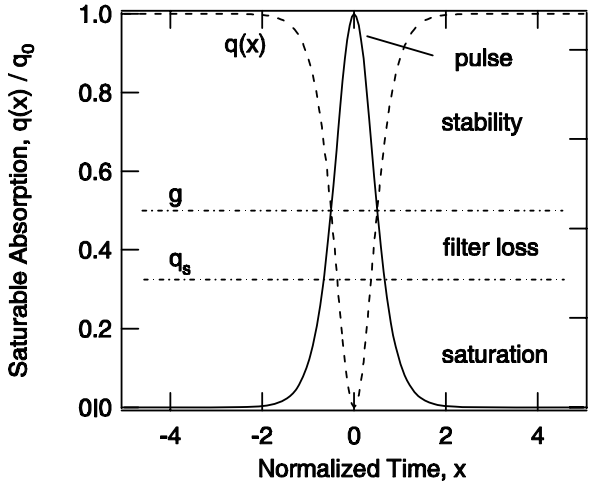

Figure 7.37: Gain and loss in a passively modelocked laser using a fast saturable absorber on a normalized time scale $x = t/\tau$. The absorber is assumed to saturate linearly with intensity according to $q(A) = q_0\left(1 - \frac{|A|^2}{A_0^2}\right)$.

Here, we assumed that the absorber saturates linearly with intensity up to a maximum value $q_0 = \gamma A_0^2$. If this maximum saturable absorption is completely exploited, see Figure 7.38.

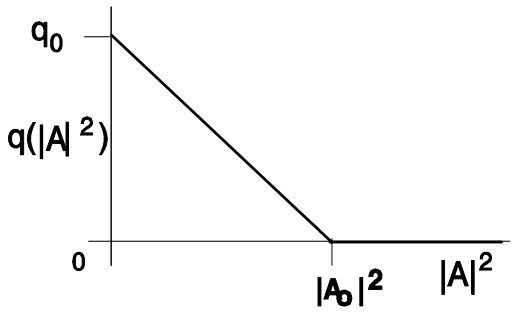

Figure 7.38: Saturation characteristic of an ideal saturable absorber

The minimum pulse width achievable with a given saturable absorption q_0 results from Eq.(7.93)

$$\frac{D_f}{\tau^2} = \frac{q_0}{2}, \tag{7.99}$$

to be

$$\tau = \sqrt{\frac{2}{q_0}} \frac{1}{\Omega_f}. \tag{7.100}$$

Note that in contrast to active modelocking the achievable pulse width is now scaling with the inverse gain bandwidth. This gives much shorter pulses. Figure 7.37 can be interpreted as follows: In steady state, the saturated gain is below loss, by about one half of the exploited saturable loss before and after the pulse. This means that there is net loss outside the pulse, which keeps the pulse stable against growth of instabilities at the leading and trailing edge of the pulse. If there is stable mode-locked operation, there must always be net loss far away from the pulse, otherwise, a continuous wave signal running at the peak of the gain would experience more gain than the pulse and would break through. From Eq.(7.93) it follows, that one third of the exploited saturable loss is used up during saturation of the aborber and actually only one sixth is used to overcome the filter losses due to the finite gain bandwidth. Note, there is a limit to the mimium pulse width. This limit is due to the saturated gain (7.94), $g_s = l + \frac{1}{2}q_0$. Therefore, from

Eq.(7.100), if we assume that the finite bandwidth of the laser is set by the gain, i.e. $D_f = D_g = \frac{g}{\Omega_g^2}$, we obtain for $q_0 \gg l$

$$\tau_{\min} = \frac{1}{\Omega_g} \tag{7.101}$$

for the linearly saturating absorber model. This corresponds to mode locking over the full bandwidth of the gain medium, as for a sech-shaped pulse, the time-bandwidth product is 0.315, and therefore,

$$\Delta f_{FWHM} = \frac{0.315}{1.76 \cdot \tau_{\min}} = \frac{\Omega_g}{1.76 \cdot \pi}. \tag{7.102}$$

As an example, for the Ti:sapphire laser this corresponds to $\Omega_g = 240$ THz, $\tau_{\min} = 3.7$ fs, $\tau_{FWHM} = 6.5$ fs, which is in good agreement with experimentally observed results [19].

This concludes the introdcution into ultrashort pulse generation by mode locking.

Bibliography

[1] R. W. Hellwarth, Eds., Advances in Quantum Electronics, Columbia Press, New York (1961).

[2] A. E. Siegman, "Lasers," University Science Books, Mill Valley, California (1986).

[3] O. Svelto, "Principles of Lasers," Plenum Press, NY 1998.

[4] http://www.llnl.gov/nif/library/aboutlasers/how.html

[5] T. H. Maimann, "Stimulated optical radiation in ruby", Nature **187**, 493-494, (1960).

[6] B.E.A. Saleh and M.C. Teich, "Fundamentals of Photonics," John Wiley and Sons, Inc., 1991.

[7] M. J. Weber, "Handbook of Lasers", CRC Press, 2000.

[8] A. Javan, W. R. Bennett and D. H. Herriott, "Population Inversion and Continuous Optical Maser Oscillation in a Gas Discharge Containing a He-Ne Mixture," Phys. Rev. Lett. **6,** (1961).

[9] W. R. Bennett, Applied Optics, Supplement 1, Optical Masers, 24, (1962).

[10] W. Koechner, "Solid-State Lasers," Springer Verlag (1990).

[11] R F Kazarinov and R A Suris, "Amplification of electromagnetic waves in a semiconductor superlattice," Sov. Phys. Semicond. **5**, p. 707 (1971).

[12] J. Faist, F. Capasso, D. L. Sivco, C. Sirtori, A. L. Hutchinson, A. Y. Cho, "Quantum cascade laser," Science **264**, p. 553 (1994).

[13] B. S. Williams, H. Callebaut, S. Kumar, Q. Hu and J. L. Reno, "3.4-THz quantum cascade laser based on longitudinal-optical-phonon scattering for depopulation," Appl. Phys. Lett. **82**, p. 1015-1017 (2003).

[14] D. Kopf, F. X. Kärtner, K. J. Weingarten, M. Kamp, and U. Keller, "Diode-pumped mode-locked Nd:glass lasers with an antiresonant Fabry-Perot saturable absorber," Optics Letters **20**, p. 1169 (1995).

[15] J. J. Zayhowski, C. Dill, "Diode-pumped passively Q-switched picosecond microchip lasers," Opt. Lett. **19**, pp. 1427 – 1429 (1994).

[16] D. J. Kuizenga and A. E. Siegman, "FM and AM modelocking of the homogeneous laser - part I: theory," IEEE J. Qunat. Electron. **6**, pp. 694 – 701 (1970).

[17] H. A. Haus, "A Theory of Forced Mode Locking", IEEE Journal of Quantum Electronics **QE-11**, pp. 323 - 330 (1975).

[18] H. A. Haus, "Theory of modelocking with a fast saturable absorber," J. Appl. Phys. **46**, pp. 3049 – 3058 (1975).

[19] R. Ell, U. Morgner, F.X. Kärtner, J.G. Fujimoto, E.P. Ippen, V. Scheuer, G. Angelow, T. Tschudi: Generation of 5-fs pulses and octave-spanning spectra directly from a Ti:Sappire laser, Opt. Lett. **26**, 373-375 (2001)